

# Nanoscale

Accepted Manuscript



This is an *Accepted Manuscript*, which has been through the Royal Society of Chemistry peer review process and has been accepted for publication.

*Accepted Manuscripts* are published online shortly after acceptance, before technical editing, formatting and proof reading. Using this free service, authors can make their results available to the community, in citable form, before we publish the edited article. We will replace this *Accepted Manuscript* with the edited and formatted *Advance Article* as soon as it is available.

You can find more information about *Accepted Manuscripts* in the [Information for Authors](#).

Please note that technical editing may introduce minor changes to the text and/or graphics, which may alter content. The journal's standard [Terms & Conditions](#) and the [Ethical guidelines](#) still apply. In no event shall the Royal Society of Chemistry be held responsible for any errors or omissions in this *Accepted Manuscript* or any consequences arising from the use of any information it contains.

Cite this: DOI: 10.1039/c0xx00000x

www.rsc.org/xxxxxx

**Paper**

# Excellent Anti-fogging Dye-sensitized Solar Cells Based On Superhydrophilic Nanoparticle Coatings

Jung Tae Park,<sup>a,b</sup> Jong Hak Kim<sup>a\*</sup> and Daeyeon Lee<sup>b\*</sup>

5 **Received (in XXX, XXX) Xth XXXXXXXXXX 20XX, Accepted Xth XXXXXXXXXX 20XX**  
DOI: 10.1039/b000000x

We present a facile method for producing anti-fogging (AF) and anti-reflection (AR) functionalized photoanodes *via* one-step SiO<sub>2</sub> nanoparticle coating for high performance solid state dye-sensitized solar cells (ssDSSCs). The AF and AR coating functionalized photoanodes are prepared by spin-coating of partially aggregated SiO<sub>2</sub> colloidal solution. Poly((1-(4-ethenylphenyl) methyl)-3-butyl-  
10 imidazolium iodide) (PEBII), prepared *via* free radical polymerization, is used as a solid electrolyte in I<sub>2</sub>-free ssDSSCs. We systematically investigate the enhanced light harvesting characteristics of AF and AR coating functionalized photoanode-based ssDSSCs by measuring UV-visible spectroscopy, incident photon-to-electron conversion efficiency (IPCE) curves under a fogging condition. Compared with a conventional photoanode based ssDSSCs, the AF and AR coating functionalized photoanodes substantially suppresses fogging and reduces reflection, leading to significantly enhanced light harvesting, especially under fogging conditions. ssDSSCs made  
15 with AF and AR coating functionalized photoanodes exhibit improved photovoltaic efficiency of 6.0 % and 5.9 % under non-fogging and fogging conditions, respectively, and retained their device efficiencies for at least 20 days, which is significant improvement of ssDSSCs with conventional photoanode (4.7 % and 1.9 % for non-fogging and fogging conditions, respectively). We believe that AF and AR functionalization *via* one-step SiO<sub>2</sub> colloidal coating is a promising method for enhancing light harvesting properties in various solar energy conversion applications.

20

## 1. Introduction

Due to their low cost and ease of preparation as well as significant potential for large area device fabrication, dye-sensitized solar cells (DSSCs) have emerged as one of the most  
25 promising alternatives to conventional silicon based p-n junction solar cells.<sup>[1-2]</sup> DSSCs are typically made by depositing a dye-sensitized wide band gap semiconductor on the surface of a transparent conductive oxide (TCO) substrate as the photoanode, a redox iodide/triiodide redox electrolyte couple and a Pt coated  
30 TCO substrate as the counterelectrode. Upon light absorption by the sensitizer, photogenerated electrons are injected from the excited dye into the conduction band of a wide band gap semiconductor, and subsequently the injected electron diffuses through the TCO substrate, while the oxide dye sensitizer is  
35 regenerated *via* reduction of the iodide/triiodide electrolyte. The oxidized redox electrolyte couple is reduced at the Pt-coated counterelectrode, completing the circuit to generate electricity from solar illumination. Recently, the drawbacks related to the use of liquid electrolytes such as leakage and evaporation has  
40 been addressed by the introduction of solid-state electrolytes based on polymers.<sup>[3-6]</sup> In addition, numerous investigations have been carried out to develop novel materials such as photonic structures and anti-reflection coatings to enhance the light harvesting performance of solid-state DSSCs (ssDSSCs).<sup>[7-20]</sup>

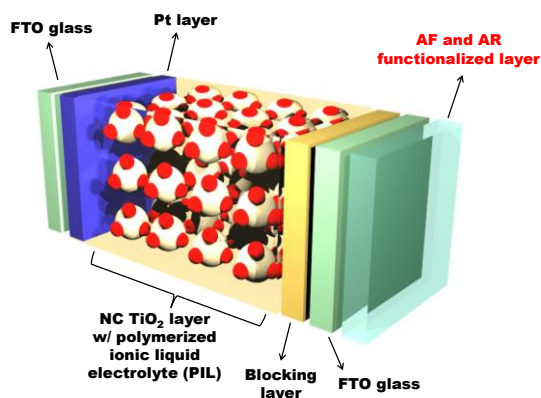
45 Although it has not been addressed extensively, one mechanism that can substantially reduce the performance of various solar cells including DSSCs is the formation of fog on the surface of the device. Fogging on transparent surfaces such as TCO substrates occurs due to the condensation of water vapor  
50 from warm and humid air onto cool surfaces, leading to the formation of micron scale water droplets on the surface. Such water droplets on the surface of solar cells (e.g., DSSCs) would induce light scattering and significantly reduce the amount of photon that could reach the light absorbing components of the  
55 devices (e.g., sensitizer in DSSCs). Fogging especially can pose a serious problem in humid areas, especially during morning hours after a long night of solar cell inactivity. Interestingly, few studies have addressed this adverse effect of fogging on solar cell performance.<sup>[21]</sup> Also, the Zou group reported an effective  
60 preparation route for self-cleaning and anti-fogging coated layer based on superhydrophilic silica nanoparticle using a dip-coating method; however, the integration of such a coating into a solar cell design was not demonstrated.<sup>[22]</sup>

In this work, we report the enhancement of DSSC  
65 performance under fogging conditions using anti-fogging (AF) coating-functionalized photoanodes. Recent studies have shown that nanoporosity-driven superhydrophilicity in nanostructure oxide materials leads to superhydrophilicity, which in turn imparts excellent anti-fogging properties to the surface. By  
70 inducing complete wetting of water on the surface, condensed

water forms a thin sheet of water, rather than individual sessile droplets, reducing random scattering of light. We fabricate such a nanoporous coating by spin coating aged colloidal SiO<sub>2</sub> nanoparticle suspension [23] and test the improved efficiency of the DSSC under fogging conditions.

## 2. Results and Discussion

Nanoporous SiO<sub>2</sub> nanoparticle coatings on the non-conducting side of DSSC photoanodes are fabricated by spin coating an aged SiO<sub>2</sub> solution. (Scheme 1) The aged 22 nm SiO<sub>2</sub> nanoparticle suspension is prepared by controlled aggregation under pH 7.0 at 60 °C for 2 hours. Aging colloidal SiO<sub>2</sub> suspensions under this condition activates the condensation reaction of surface silanol groups, which induces aggregation of SiO<sub>2</sub> nanoparticles. [23] A recent study has shown that SiO<sub>2</sub> nanoparticle films generated from such an aged suspension are highly porous and have anti-reflection properties, which, in itself, would be beneficial for DSSCs. [23] We adjust the spin coating condition to generate ~110 nm thick SiO<sub>2</sub> nanoparticle film, which forms a quarter wavelength single layer anti-reflection coating. (See Supporting Information). Consistent with the previous study we confirm that SiO<sub>2</sub> nanoparticle films deposited from the aged solution are thicker and more porous than those deposited from un-aged fresh SiO<sub>2</sub> suspension (Fig. 1). [24] These changes in the structure of the SiO<sub>2</sub> nanoparticle film are believed to be due to the formation of nanoparticle aggregates upon aging. [23] Also, no macroscopic cracks or other major imperfections are seen in the SiO<sub>2</sub> nanoparticle films.



**Scheme 1.** Schematic illustration of preparation of the anti-fogging and anti-reflection functionalized photoanodes to dye-sensitized solar cells (DSSCs) using one-step SiO<sub>2</sub> colloidal coating approach.

**Table 1.** Refractive index, thickness, calculated porosity and contact angle value of SiO<sub>2</sub> nanoparticle solution coatings as a function of aging condition on non-conducting side of FTO substrate.<sup>a</sup>

Aging condition	Refractive Index	Thickness	Porosity	Contact Angle
un-aged	1.33 ± 0.02	77 ± 5 nm	0.32 ± 0.05	Not measured
2 hour, 60oC	1.26 ± 0.02	107 ± 5 nm	0.48 ± 0.05	3 °

<sup>a</sup> Contact angle of non-conducting side of FTO substrate without SiO<sub>2</sub> nanoparticle solution is 50 °.

We first evaluate the wetting properties of the non-conducting side of un-treated and SiO<sub>2</sub> nanoparticle-coated fluorine-doped tin oxide (FTO) glasses. We note that all of the SiO<sub>2</sub> nanoparticle coatings below are generated from the aged SiO<sub>2</sub> suspension. Fogging on the FTO glasses is induced by exposing them to high humid environments after cooling them at a low temperature (< 0 °C). The contact angle of a water droplet on the non-conducting side of conventional photoanode without any treatment is 50 °, whereas that on the non-conducting side of SiO<sub>2</sub> nanoparticle coated photoanode is only 3 ° as shown in Fig. 2 and summarized in Table 1. The superhydrophilicity of the aged SiO<sub>2</sub> nanoparticle coating is due to the nanowicking of water into the network of the capillaries in the nanoparticle assembly, which induces complete sheeting of water. [25,26] Therefore, these results strongly indicate that these one-step SiO<sub>2</sub> colloidal coating could serve as highly effective anti-fogging (AF) coatings.

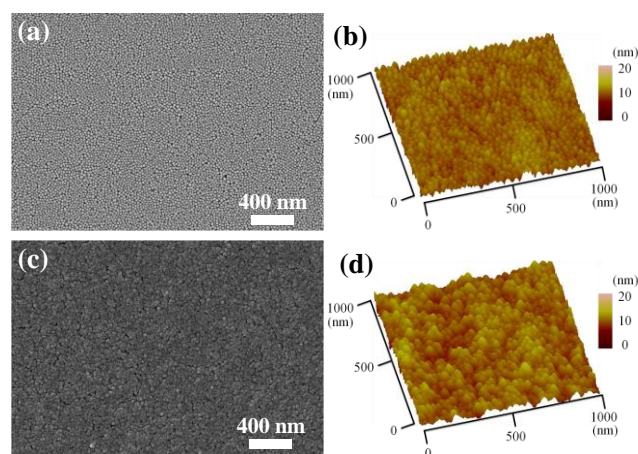


**Figure 1.** FE-SEM surface image (a) and tapping mode AFM three-dimensional height image (b) of SiO<sub>2</sub> nanoparticle coatings on FTO substrates from aged (via 2 hour, 60 °C condition) SiO<sub>2</sub> suspension, respectively. FE-SEM surface image (c) and tapping mode AFM three-dimensional height image (d) of SiO<sub>2</sub> nanoparticle coatings on FTO substrates from un-aged fresh SiO<sub>2</sub> suspension, respectively.

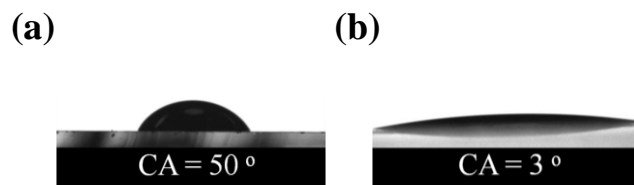


**Figure 2.** Images of water contact angle on non-conducting side of FTO substrate without (a) and with (b) SiO<sub>2</sub> nanoparticle coating, respectively.

We test the effect of SiO<sub>2</sub> nanoparticle on the transmission of visible light through under the fogging condition. SiO<sub>2</sub> nanoparticle-functionalized FTO glass (top) gives a much higher transmittance as compared to the reference FTO glass (bottom)

under the fogging condition, as shown in **Fig. 3 (a)**. These results indicate that a large area anti-fogging coating can be readily prepared on transparent surfaces such as FTO glass with a high degree of uniformity by spin coating of aged SiO<sub>2</sub> nanoparticle suspensions. The high transmissivity of the SiO<sub>2</sub> nanoparticle functionalized FTO glass is also confirmed by UV-Vis spectroscopy (**Fig. 3 (b)**). It can be seen that fogging on the SiO<sub>2</sub> nanoparticle-functionalized FTO glass is considerably suppressed over the entire visible range when compared to that on the conventional photoanode outer surface. We also confirm the anti-reflection property of the SiO<sub>2</sub> colloidal coating enhances the light transmission through the FTO glass under non-fogging conditions as shown in **Fig. 3 (c, d)**, which again will be beneficial for increasing the light harvesting of DSSCs.

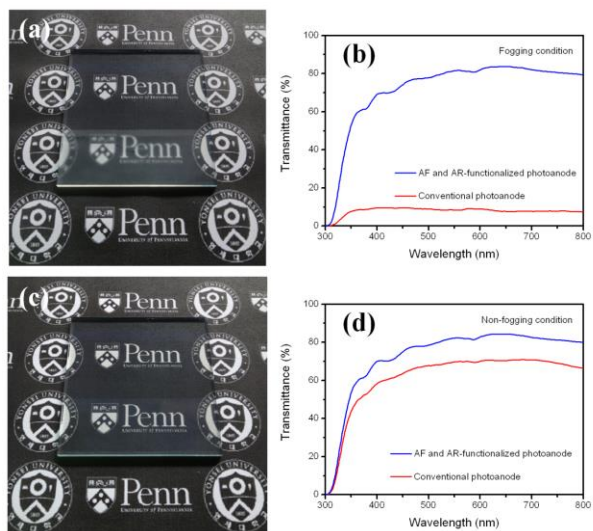


**Figure 3.** (a) photograph of a untreated FTO glass (bottom) and a SiO<sub>2</sub> nanoparticle-coated FTO glass (top) under fogging condition (b) transmittance spectra in the visible region for untreated and SiO<sub>2</sub> nanoparticle-coated FTO glasses under fogging condition, respectively. (c) photograph of a untreated FTO glass (bottom) and a SiO<sub>2</sub> nanoparticle-coated FTO glass (top) under non-fogging, (d) transmittance spectra in the visible region for untreated and SiO<sub>2</sub> nanoparticle-coated FTO glasses under non-fogging condition, respectively.

We fabricate and compare the performance of DSSCs with and without SiO<sub>2</sub> nanoparticle coating on the non-conducting side of the photoanodes under a fogging condition, which is induced by breathing on the surface of DSSCs under a humid condition (> 80% relative humidity). We fabricate ssDSSCs by using poly(1-((4-ethenylphenyl)methyl)-3-butyl-imidazolium iodide) (PEBII) as the solid electrolyte. As a reference point, ssDSSCs with SiO<sub>2</sub> nanoparticle coatings have a conversion efficiency of 6.0% under the non-fogging condition (See next **Fig. 6**). Fogging on the control devices that are made of untreated photoanodes causes a significant performance degradation as seen in **Fig. 4 (a)** and **Table 2**. A power conversion efficiency ( $\eta$ ) of 1.9% is attained for the conventional photoanode based ssDSSCs with  $V_{oc}$  of 0.85 V,  $J_{sc}$  of 4.1 mA/cm<sup>2</sup>, and  $FF$  of 0.55 due to the loss of light via scattering on the foggy FTO surface. In contrast, the AF and AR-

coating functionalized photoanode-based ssDSSCs achieve  $V_{oc}$  of 0.84 V,  $J_{sc}$  of 14.1 mA/cm<sup>2</sup>, and  $FF$  of 0.54, which results in an  $\eta$  of 5.9%. These values represent close to 220% and 210% enhancements in  $J_{sc}$ , and  $\eta$  as compared to the ssDSSCs without AF- and AR- coatings characterized under the fogging condition. Interestingly, the  $V_{oc}$  and  $FF$  of the ssDSSC remain almost unchanged under the fogging condition for the AF and AR-coating functionalized photoanode-based ssDSSCs when compared to the conventional photoanode based ssDSSCs. These results indicate that SiO<sub>2</sub> nanoparticle coating on the non-conducting side of the photoanode does not affect the internal electrochemical processes in the ssDSSCs such as recombination or electron back reaction at the electrolyte/electrode interface.<sup>[24]</sup> Similar results were also observed for DSSCs modified with highly reflective counter electrodes, which were prepared through the deposition of alternating layers of organized mesoporous TiO<sub>2</sub> and colloidal SiO<sub>2</sub> nanoparticles on the non-conducting side of the counter electrode.<sup>[27]</sup>

The IPCE efficiency of the ssDSSCs with the SiO<sub>2</sub> nanoparticle-coating functionalized photoanode is also considerably greater than those with un-treated photoanodes in the entire visible region as seen in **Fig. 4 (b)**. These improved  $J_{sc}$  values as well as the IPCE efficiency result from the enhanced transmittance and higher light harvesting characteristics of the photoanode under the fogging.

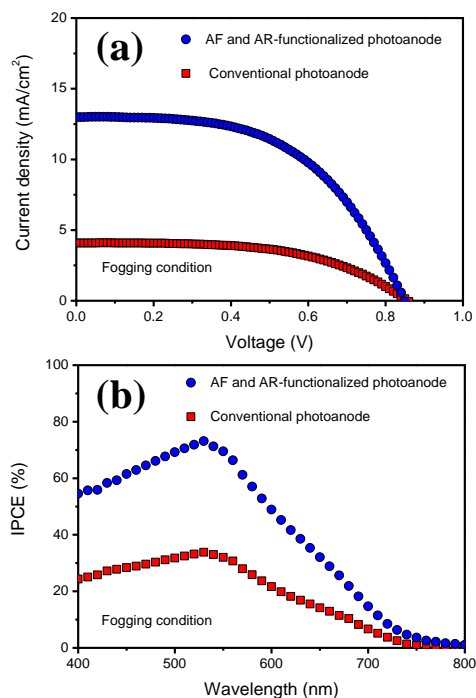


**Figure 4.** (a) Photocurrent density-photovoltaic ( $J$ - $V$ ) and (b) IPCE curves under fogging condition for ssDSSC fabricated with untreated photoanode and aged SiO<sub>2</sub> nanoparticle-coated photoanodes at 100 mW/cm<sup>2</sup>.

The long-term performance of SiO<sub>2</sub> nanoparticle coating in preventing fogging on ssDSSCs is tested by keeping the device in a dark condition and then measuring the device performance under fogging condition every 24 hours as shown in Fig. 5. The superhydrophilicity of the nanoparticle coating is maintained at least for 20 days, and the device efficiency shows negligible reduction during such a period when tested under the fogging condition.

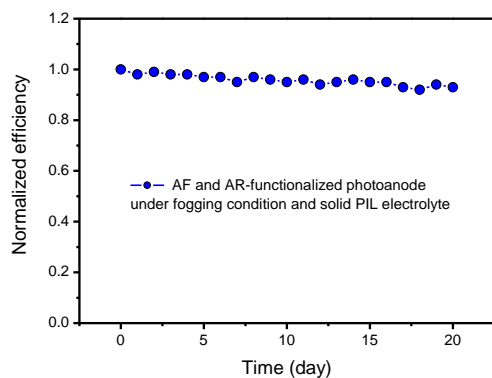


Figure 5. Normalized cell efficiency of the ssDSSCs with SiO<sub>2</sub> nanoparticle-functionalized photoanodes. (40-50 % relative humidity).

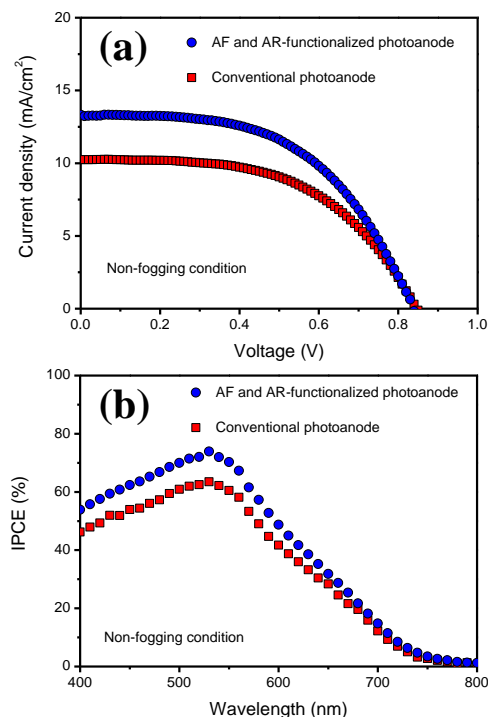


Figure 6. (a) Photocurrent density-photovoltaic ( $J$ - $V$ ) and (b) IPCE curves under the non-fogging condition for ssDSSC fabricated with untreated photoanode and aged SiO<sub>2</sub> nanoparticle-coated photoanodes at 100 mW/cm<sup>2</sup>.

In addition, to examine the effects of the one-step SiO<sub>2</sub> colloidal coating on the light harvesting properties of ssDSSCs under non-fogging conditions, we fabricate ssDSSCs with untreated photoanode and aged SiO<sub>2</sub> nanoparticle deposited photoanode and compare the photovoltaic parameters, *i.e.*, open-circuit voltage ( $V_{OC}$ ), short-circuit photocurrent density ( $J_{sc}$ ), fill factor ( $FF$ ), and light to electricity conversion efficiency ( $\eta$ ), as shown in Fig. 6 (a), Table 2 lists the photovoltaic parameters of these two ssDSSCs. Here, we note that the anti-reflection property of the SiO<sub>2</sub> nanoparticle coating is also extremely beneficial for DSSCs because the coating significantly enhances the device efficiency under non-fogging conditions by suppressing the reflection at the non-conducting side of the photoanode. The  $\eta$  of the SiO<sub>2</sub> nanoparticle-functionalized photoanode based ssDSSCs reaches 6.0 % at 100 mW/cm<sup>2</sup>, which is a relatively high value among for N719 sensitizer-based ssDSSCs [28-33] and is 1.3-fold higher than the device efficiency of ssDSSC with no AR- and AF-coatings. In particular, it can be seen that the  $J_{sc}$  in the AF and AR functionalized photoanode based ssDSSCs (13.3 mA/cm<sup>2</sup>) are considerably higher than that for the untreated photoanode system (10.2 mA/cm<sup>2</sup>) under the non-fogging condition, whereas the  $V_{oc}$ ,  $FF$  are not affected by the one-step SiO<sub>2</sub> colloidal coating layer, indicating enhanced light harvesting. IPCE measurements as a function of wavelength from 400 to 800 nm are also carried out under non-fogging condition for ssDSSCs with and without SiO<sub>2</sub> nanoparticle coatings, as shown in Fig. 6 (b). The IPCE spectra under non-fogging condition show that the ssDSSCs with nanoparticle coated photoanodes show higher  $\eta_{IPCE}$  compared to the ssDSSC based on untreated photoanodes over the entire visible spectrum region. The enhancement of the  $\eta_{IPCE}$  for the SiO<sub>2</sub> nanoparticle-functionalized photoanode based ssDSSCs results from the suppression of reflection and in turn increased transmittance of light through the TCO glass.

Table 2. Photovoltaic parameters of untreated photoanode and SiO<sub>2</sub> nanoparticle-coated photoanode based ssDSSCs. Solid PIL electrolyte is used for ssDSSC fabrication (PEBII, poly(1-((4 ethenylphenyl)methyl)-3-butyl-imidazolium iodide)).

Photoanode	Condition	$V_{oc}$ (V)	$J_{sc}$ (mA/cm <sup>2</sup> )	$FF$	$\eta$ (%)
Conventional	Non-fogging	0.84	10.2	0.54	4.7
	Fogging	0.85	4.1	0.55	1.9
AF and AR-functionalized	Non-fogging	0.83	13.3	0.54	6.0
	Fogging	0.84	13.0	0.54	5.9

We also observe similar enhancement effects under the fogging, non-fogging condition when liquid electrolytes are used for DSSC fabrication as shown in Fig. 7 (a,b) and Table 3; that is, the application of the SiO<sub>2</sub> nanoparticle film on the non-conducting side of the photoanode minimizes the performance degradation under the fogging, non-fogging condition.

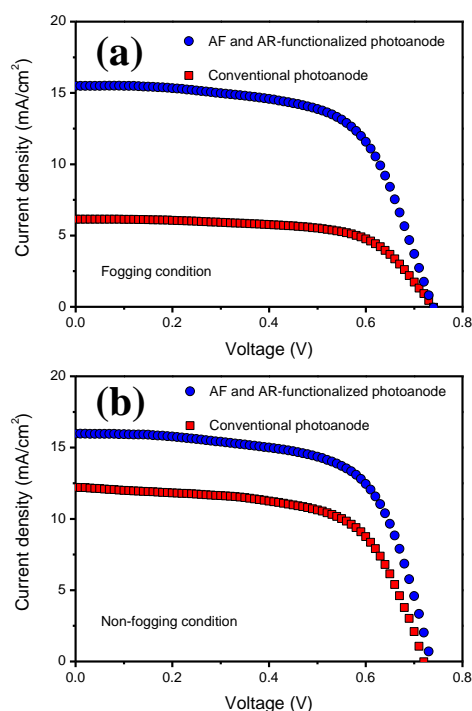


**Figure 7.** (a) Photocurrent density-photovoltaic ( $J$ - $V$ ) curves under fogging condition and (b) non-fogging condition for liquid electrolyte-based DSSCs using untreated and SiO<sub>2</sub> nanoparticle-coated photoanodes at 100 mW/cm<sup>2</sup>.

**Table 3.** Photovoltaic parameters of liquid electrolyte-based DSSCs with untreated and SiO<sub>2</sub> nanoparticle-coated photoanodes. 1-butyl-3-methylimidazolium iodide/I<sub>2</sub>/guanidinium thiocyanate/4-tert-butylpyridine in acetonitrile and valeronitrile is used as the liquid electrolyte.

Photoanode	Condition	$V_{oc}$ (V)	$J_{sc}$ (mA/cm <sup>2</sup> )	$FF$	$\eta$ (%)
Conventional	Non-fogging	0.71	12.2	0.64	5.5
	Fogging	0.73	6.1	0.65	2.9
AF and AR-functionalized	Non-fogging	0.73	16.0	0.65	7.6
	Fogging	0.73	15.5	0.64	7.2

### 3. Conclusions

In summary, we have shown that fogging can significantly degrade the performance of a DSSC and that such a detrimental effect can be significantly eliminated by depositing superhydrophilic SiO<sub>2</sub> nanoparticle coating on the non-conducting side of the DSSC photoanode. While the conversion efficiencies of DSSCs with untreated photoanodes under the fogging condition are reduced by 47 and 60 % for liquid and solid electrolyte-containing devices, respectively, the losses in the efficiency for devices with the nanoparticle coatings were less

than 2 and 6 %, respectively. In addition, these nanoparticle coatings impart anti-reflection properties to the TCO glass, increasing the light transmission through and, in turn, enhancing the performance of the DSSCs under non-fogging conditions. We believe this one-step SiO<sub>2</sub> colloidal coating approach for improved light harvesting property is a simple, rapid and inexpensive process that can be widely used in a variety of photoelectrochemical devices to enhance solar energy conversion.

## 4. Experimental Section

### Material

LUDOX TM-40 (40 wt% SiO<sub>2</sub> suspension in H<sub>2</sub>O, 22 nm), titanium(IV) bis(ethyl acetoacetato) diisopropoxide, 1-butylimidazole, 4-chloromethylstyrene, lithium iodide (LiI), magnesium sulfate (MgSO<sub>4</sub>), 2,2'-azobisisobutyronitrile (AIBN), iodine (I<sub>2</sub>), 3-methoxypropionitrile, butylmethylimidazolium iodide, guanidinium thiocyanate, 4-tertbutylpyridine, valeronitrile, and chloroplatinic acid hexahydrate (H<sub>2</sub>PtCl<sub>6</sub>) were purchased from Sigma-Aldrich (St Louis, MO). 2-propanol, chloroform, butanol, ethanol, diethylether and ethyl acetate were purchased from J.T. Baker. Deionized water (>18 MΩ·m) was obtained with a water purification system made by Millipore Corporation. Ruthenium dye (535-bisTBA, N719), TiO<sub>2</sub> colloidal paste (Ti-Nanoxide, D20), and 60 μm thick Surlyn were purchased from Solaronix, Switzerland. Fluorine-doped tin oxide (FTO) conducting glass substrate (TEC8, 8 ohms/sq, 2.3 mm thick) was purchased from Pilkington, France. All chemicals and solvents reagents used in our experiments were obtained from commercial sources as guaranteed grade reagents and used without further purification.

### Preparation of SiO<sub>2</sub> colloidal solution for anti-fogging and anti-reflection coating-functionalized photoanode (AF and AR-functionalized photoanode)

SiO<sub>2</sub> colloidal solutions were prepared by slightly modifying a previously reported method.<sup>[23]</sup> For solutions that were aged, LUDOX TM-40 (40 wt% SiO<sub>2</sub> suspension in H<sub>2</sub>O, 22 nm in size) was adjusted to pH 7.0 by using HCl and the solution was aged for 3 h at 60 °C. This process was required to reduce the negative surface charge on the SiO<sub>2</sub> nanoparticles and produce particle aggregation through condensation process of silanol groups (-OH) on the SiO<sub>2</sub> nanoparticle surface. This solution was subsequently diluted to 5 wt% for spin coating.

### Preparation of AF and AR-functionalized photoanode

Transparent fluorine-doped tin oxide (FTO) conducting glass substrate was employed in order to prepare the AF and AR-coating functionalized photoanodes. Before fabricating AF and AR coating onto the non-conducting side of the photoanode, the FTO glass substrates were rinsed with 2-propanol and chloroform each for 30 min and dried under nitrogen, respectively. Subsequently, a dense TiO<sub>2</sub> film as a blocking layer on the conducting side of FTO substrate was prepared by spin coating a titanium(IV) bis(ethyl acetoacetato) diisopropoxide solution (2 wt% in butanol) at 1500 rpm for 10 sec, followed by calcination at 50 °C for 30 min and subsequently calcined at 450 °C for 30

min. Next, to prepare nanocrystalline TiO<sub>2</sub> layers, we blade-coated the commercial TiO<sub>2</sub> paste (commercially known as Ti-Nanoxide, D20) on top of the blocking layer on the conducting side of the FTO substrate. The FTO glass was subsequently heated to 450 °C for 30 min. And then, as prepared photoanode was sensitized with 0.5 mM ruthenium complex, cis-diisothiocyanato-bis(2,2'-bipyridyl-4,4'-dicarboxylato) ruthenium(II) bis(tetrabutylammonium), (commercially known as N719) in ethanol for 24 hours. The aged SiO<sub>2</sub> colloidal solution was spin coated onto the non-conducting side of the photoanode at 2000 rpm and were dried at 70 °C for 30 min.

#### Fabrication of ssDSSCs and DSSCs

For fabrication of solid-state dye-sensitized solar cells (ssDSSCs) and dye-sensitized solar cells (DSSCs), the polymerized ionic liquid (PIL) and liquid state electrolyte solution was dropped onto the photoanode and covering with the counterelectrode, according to previous reported procedure, respectively.<sup>[34,35]</sup> For the ssDSSCs system, a PIL, *i.e.*, poly(1-(4-ethenylphenyl)methyl)-3-butyl-imidazolium iodide) (PEBII) electrolyte was prepared by dissolving in acetonitrile. And then, the PIL electrolyte solution was allowed to infiltrate the photoanode. The photoanode was subsequently placed on top of the counter electrode. In the case of DSSCs, a liquid electrolyte, *i.e.*, 1-butyl-3-methylimidazolium iodide, iodine (I<sub>2</sub>), guanidinium thiocyanate, and 4-tert-butylpyridine (TBP) solution was prepared by dissolving in acetonitrile and valeronitrile (v/v, 85:15). And then, DSSCs were filled with a liquid electrolyte solution through a drilled hole on the counterelectrode. The gap between the two electrodes was maintained at 60 μm using a thick Surlyn tape.

#### Characterization

The surface morphology of SiO<sub>2</sub> nanoparticle coated photoanodes were observed using a Field emission-scanning electron microscope (SUPRA 55VP, Carl Zeiss). Tapping mode atomic force microscopy (TM-AFM) (Nanoscope IV, Digital Instruments) was used to examine the topology of nanoparticle-coated FTO glasses. Thickness and refractive index of nanoparticle coatings were determined using a spectroscopic ellipsometer, Alpha-SE, and the Complete EASE software package (J.A. Woollam). Transmittance spectroscopy was measured with a spectrophotometer (Hewlett Packard) in the range 300 to 800 nm. The incident photon to current conversion efficiency (IPCE) was measured as a function of wavelength from 400 to 800 nm using a specially designed IPCE system for dye-sensitized solar cells (K3100). The photocurrent density-voltage (*J-V*) characteristics of the devices were measured using a Keithley 2400 source under illumination by an AM1.5G A class solar simulator (ABET Technologies, model 11000) at 100 mW/cm<sup>2</sup>, referenced to a standard silicon cell. The UV-Vis absorption spectra were measured by a JASCO 550A spectrometer. During photocurrent density-voltage measurement, the DSSCs were covered with a black mask with an aperture to avoid additional light coming through lateral space. The photoelectrochemical performances were calculated by the following equations.

$$FF = V_{max} \cdot J_{max} / Voc \cdot Jsc \quad (1)$$

$$\eta = V_{max} \cdot J_{max} / Pin \cdot 100 = Voc \cdot Jsc \cdot FF / Pin \cdot 100 \quad (2)$$

where *Jsc* is a short-circuit current density (mA/cm<sup>2</sup>), *Voc* is an open-circuit voltage (V), *Pin* is an incident light power, *FF* is the fill factor,  $\eta$  is an overall energy conversion efficiency and *J<sub>max</sub>* (mA/cm<sup>2</sup>) and *V<sub>max</sub>* (V) are the current density and voltage in the *J-V* curve, respectively, at the point of maximum power output. The wettability of nanoparticle-coated FTO glasses was characterized by the measurement of water contact angles on their surfaces (FM 40, KRUSS Gmbh Germany). The volume of the distilled water droplet use for contact angle determination was 10 μl.

#### Acknowledgements

This work is supported by NSF CBET-1234993, NSF DMR-1055594, the Penn MRSEC (DMR-1120901), the Active Polymer Center for Pattern Integration (R11-2007-050-00000-0) and the Core Research Program (2012R1A2A2A02011268).

#### Notes and references

- <sup>a</sup> Department of Chemical and Biomolecular Engineering, Yonsei University, 50 Yonsei-ro, Seodaemun-gu, Seoul 120-749, South Korea  
<sup>b</sup> Department of Chemical and Biomolecular Engineering, University of Pennsylvania, 220 South 33rd Street, Philadelphia, Pennsylvania 19104, USA  
 E-mail: jonghak@yonsei.ac.kr, daeyeon@seas.upenn.edu
- † Electronic Supplementary Information (ESI) available: [details of any supplementary information available should be included here]. See DOI: 10.1039/b000000x/
- [1] B. O'Regan, M. Gratzel, *Nature* 1991, **353**, 737.
  - [2] A. Yella, H.-W. Lee, H. N. Tsao, C. Yi, A. K. Chandiran, M. K. Nazeeruddin, E. W.-G. Diao, C. Y. Yeh, S. M. Zakeeruddin, M. Gratzel, *Science* 2011, **334**, 629.
  - [3] G. Wang, L. Wang, S. Zhuo, S. Fang, Y. Lin, *Chem. Commun.* 2011, **47**, 2700.
  - [4] Y.-H. Chang, P.-Y. Lin, S.-R. Huang, K.-Y. Liu, K.-F. Lin, *J. Mater. Chem.* 2012, **22**, 15592.
  - [5] S. Yanagida, Y. H. Yu and K. Manseki, *Acc. Chem. Res.*, 2009, **42**, 1827.
  - [6] T. Leijtens, I.-K. Ding, T. Giovenzana, J.T. Bloking, M.D. McGehee, A. Sellinger, *ACS Nano*, 2012, **6**, 1455.
  - [7] L. Yang, W. W.-F. Leung, *Adv. Mater.* 2013, **25**, 1792.
  - [8] S. Nejadi, K. K. S. Lau, *Nano Lett.* 2011, **11**, 419.
  - [9] T. Chen, L. Qiu, Z. Cai, F. Gong, Z. Yang, Z. Wang, H. Peng, *Nano Lett.* 2012, **12**, 2568.
  - [10] M. Shanmugam, R. Jacobs-Gedrim, C. Durcan, B. Yu, *Nanoscale*, 2013, **5**, 11275.
  - [11] L. Yi, Y. Liu, N. Yang, Z. Tang, H. Zhao, G. Ma, Z. Su, D. Wang, *Energy Environ. Sci.* 2013, **6**, 835.
  - [12] G. Shang, J. Wu, S. Tang, M. Huang, Z. Lan, Y. Li, J. Zhao, X. Zhang, *J. Mater. Chem.* 2012, **22**, 25335.
  - [13] J. D. Roy-Mayhew, D. J. Bozym, C. Punckt, I. A. Aksay, *ACS Nano*, 2010, **4**, 6203.

- [14] Z. Dong, H. Ren, C. M. Hessel, J. Wang, R. Yu, Q. Jin, M. Yang, Z. Hu, Y. Chen, Z. Tang, H. Zhao, D. Wang, *Adv. Mater.* 2014, **26**, 905.
- [15] H. Wang, K. Sun, F. Tao, D. J. Stacchiola, Y. H. Hu, *Angew. Chem. Int. Ed.* 2013, **52**, 9210.
- [16] C.-Y. Wu, Y.-T. Liu, P.-C. Huang, T.-J. M. Luo, C.-H. Lee, Y.-W. Yang, T.-C. Wen, T.-Y. Chen, T.-L. Lin, *Nanoscale*, 2013, **5**, 9181.
- [17] S.-H. Chang, M.-D. Lu, Y.-L. Tung, H.-Y. Tuan, *ACS Nano*, 2013, **7**, 9443.
- [18] L.-K. Yeh, K.-Y. Lai, G.-J. Lin, P.-H. Fu, H.-C. Chang, C.-A. Lin, J.-H. He, *Adv. Energy Mater.* 2011, **1**, 506.
- [19] J. Zhu, C.-M. Hsu, Z. Yu, S. Fan, Y. Cui, *Nano Lett.* 2010, **10**, 1979.
- [20] S.Y. Heo, J.K. Koh, G. Kang, S.H. Ahn, W.S. Chi, K. Kim, J.H. Kim, *Adv. Energy Mater.* 2014, **4**, 1300632.
- [21] D. Lee, M. F. Rubner, R. E. Cohen, *Nano Lett.* 2006, **6**, 2305.
- [22] C.S. Thompson, R.A. Fleming, M. Zou, *Solar Energy Materials & Solar Cells* 2013, **115**, 108.
- [23] K.T. Cook, K.E. Tettey, R.M. Bunch, D. Lee, A. J. Nolte, *ACS Appl. Mater. Interfaces* 2012, **4**, 6426.
- [24] J.T. Park, J.H. Prosser, S.H. Ahn, S.J. Kim, J.H. Kim, D. Lee, *Adv. Funct. Mater.* 2013, **23**, 2193.
- [25] F.C. Cebeci, Z. Wu, L. Zhai, R.E. Cohen, M.F. Rubner, *Langmuir* 2006, **22**, 2856.
- [26] K. E. Tettey, M. I. Dafinone, D. Lee, *Materials Express*, 2011, **1**, 89.
- [27] J.T. Park, J.H. Prosser, D.J. Kim, J.H. Kim, D. Lee, *ChemSusChem* 2013, **6**, 856.
- [28] R.D. Costa, F. Werner, X. Wang, P. Grönninger, S. Feihl, F. T. U. Kohler, P. Wasserscheid, S. Hibler, R. Beranek, K. Meyer, D. M. Guldi, *Adv. Energy Mater.* 2013, **3**, 657.
- [29] D. Xu, H. Zhang, X. Chen, F. Yan, *J. Mater. Chem. A*, 2013, **1**, 11933.
- [30] C. Xu, J. Wu, U. V. Desai, D. Gao, *Nano Lett.* 2012, **12**, 2420.
- [31] H. Wang, J. Li, F. Gong, G. Zhou, Z.-S. Wang, *J. Am. Chem. Soc.* 2013, **135**, 12627.
- [32] S. Guldin, S. Huettner, P. Tiwana, M.C. Orilall, B. Uelguet, M. Stefik, P. Docampo, M. Kolle, G. Divitini, C. Ducati, S. A. T. Redfern, H. J. Snaith, U. Wiesner, D. Eder, U. Steiner, *Energy Env. Sci.* 2011, **4**, 225.
- [33] E.J.W. Crossland, M. Nedelcu, C. Ducati, S. Ludwigs, M.A. Hillmyer, U. Steiner, H.J. Snaith, *Nano Lett.* 2009, **9**, 2813.
- [34] J.T. Park, R. Patel, H. Jeon, D.J. Kim, J.-S. Shin, J.H. Kim, *J. Mater. Chem.* 2012, **22**, 6131.
- [35] J.T. Park, W.S. Chi, D.K. Roh, S.H. Ahn, J. H. Kim, *Adv. Funct. Mater.* 2013, **23**, 26.

## Graphical Abstract

We present a method for eliminating the negative impact of fogging on dye-sensitized solar cells using superhydrophilic nanoparticle coatings. Superhydrophilic coatings made of spin-coated  $\text{SiO}_2$  nanoparticles suppress fogging on the photoanodes of solid-state dye-sensitized solar cells and in turn significantly improves the devices efficiency under fogging conditions. We believe these one-step  $\text{SiO}_2$  colloidal coating is extremely useful for enhancing light harvesting properties of various photovoltaic and photoelectrochemical devices.

